

Model calculation of the crystal-field magnetostriction and its temperature dependence in the itinerant uniaxial ferromagnet Y_2Fe_{17}

K. Kulakowski*

Departamento de Física de Materiales, Facultad de Química, Universidad del País Vasco (Euskal Herriko Unibertsitatea), 20080 San Sebastián (Donostia), Spain

A. del Moral

Unidad de Magnetismo de Sólidos, Departamento de Física de Materia Condensada and Instituto de Ciencia de Materiales de Aragón, Universidad de Zaragoza and Consejo Superior de Investigaciones Científicas, 50009 Zaragoza, Spain

(Received 20 December 1993; revised manuscript received 14 March 1994)

The observed crystal-field magnetostriction and its complex temperature dependence have been calculated for the itinerant iron-rich uniaxial ferromagnet Y_2Fe_{17} , using a simple, although highly efficient, type of rigid-band Stoner model. We have evaluated the irreducible magnetostriction modes $\epsilon^{\alpha,1}$ and $\epsilon^{\alpha,2}$, which represent the volume and c -axis pure tetragonal strains, respectively, as well as their temperature dependencies. Good agreement with the available experimental results has been attained. As a result, values of the corresponding microscopic magnetoelastic coupling coefficients, M_{12}^{α} and M_{22}^{α} , have been obtained. Those values are very large (around -10^3 K/Fe atom), as expected for an intermetallic compound with a $3d$ shell transition element.

I. INTRODUCTION

The calculation of spontaneous magnetostriction, either of a volume or shape character, and in particular their temperature dependence, is for itinerant electron $3d$ metals and intermetallic compounds a more complex, and less well established, matter than for localized $4f$ magnetic-moment rare-earth systems. For these we dispose of the standard model of magnetoelastic (MEL) coupling of Callen and Callen,¹ which for single-ion crystal-field- (CF) origin magnetostriction, namely, predicts a monotonic decrease of the strictions with temperature. However, for $3d$ systems, as in the intermetallic Y_2Fe_{17} (Ref. 2), the striction modes depict complex temperature dependencies, and they can be null or change their sign below the Curie temperature. These facts have no simple explanation within the standard localized-moment MEL model, under the assumption of only including second-order terms in the magnetoelastic CF-origin Hamiltonian. However, nonmonotonic temperature variations of magnetostriction were also observed in rare-earth (RE) intermetallics, e.g., in RCo_5 (Ref. 3) and $R_2Fe_{14}B$ (Ref. 4), where the magnetostriction associated with the R^{3+} ion needed to be explained, the introduction of higher-order terms in the magnetoelastic-CF Hamiltonian.⁴

The calculation of magnetostriction in $3d$ metals and alloys traces to the works of Brooks, Katayama, and Fletcher (BKF model),⁵ based on the tight-binding approximation (TBA), and not much has been advanced since then except for a crucial simplification introduced by Kondorskii and Straube⁶ and Mori and co-workers.⁷ A modified version of the BKF model was recently developed⁸ to explain the approach to technical saturation of the CF magnetostriction in the hexagonal fer-

romagnet Y_2Fe_{17} (Ref. 9). The difficulty with the BKF model is the need for a good knowledge of the system band structure, and even an explanation of the nonmonotonic striction variation is unfeasible. Only a diagonalization of the full Hamiltonian in a sufficient number of k -space points would probably give the answer.

Recently a slightly more simplified but, in our opinion, quite efficient model of magnetostriction for itinerant systems was proposed,¹⁰ which allows for the calculation of the striction temperature dependence, within the rigid-band approximation. The model was then limited to amorphous isotropic¹¹ and cubic¹⁰ systems, and it has been presently extended to uniaxial ones, the case for the Y_2Fe_{17} model system.

The compound Y_2Fe_{17} crystallizes in the Th_2Ni_{17} -type hexagonal space group $P6_3/mmc$ (Refs. 12 and 13). A study of many magnetic properties of Y_2Fe_{17} can be found in Refs. 9 and 12. There are four nonequivalent Fe sites ($4f$, $6g$, $12j$, and $12k$) in the unit cell, with the $4f$ dumbbell of Fe atoms supporting the $3m$ trigonal point-group symmetry, the remainder sites being of lower symmetry.^{12,13} Within the $3d$ real atomic orbitals representation, i.e., $|xz\rangle \equiv |1\rangle$, $|yz\rangle \equiv |2\rangle$, $|xy\rangle \equiv |3\rangle$, $|x^2-y^2\rangle \equiv |4\rangle$, and $|2z^2-(x^2+y^2)\rangle \equiv |5\rangle$, all sites, except the $4f$, support singlet-based representations, being magnetostrictively inactive. For the $3m$ symmetry the fivefold orbital degeneracy is lifted into a singlet, $|5\rangle$, and two doublets, $\{|1\rangle, |2\rangle\}$ and $\{|3\rangle, |4\rangle\}$ (Ref. 1), and therefore the $4f$ Fe atoms are potentially the only magnetostrictively active. However, notice that such a levels splitting is also applicable to hexagonal symmetry systems, and we will take advantage of it when modeling the magnetostriction as a result of the whole average magnetic system.

Magnetostriction measurements, between 4.2 K and

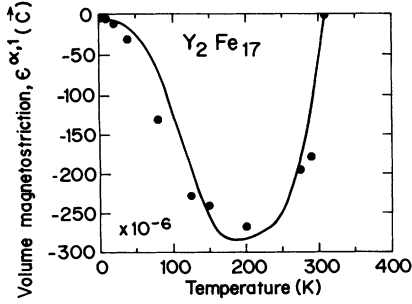


FIG. 1. Temperature dependence of the volume irreducible strain $\epsilon^{\alpha,1}$ for the hexagonal Y_2Fe_{17} intermetallic compound. The points (●) are the experimental results (Refs. 2 and 8), and the continuous line the model fit, for the microscopic magnetoelastic coupling parameter M_{12}^{α} quoted in Table I. The experimental strains correspond to having the spontaneous magnetization along the hard c axis.

near the Curie temperature, $T_C \cong 310$ K (Ref. 12), were recently performed by García-Landa *et al.*² in applied fields up to 15 T, with a determination of the field and temperature variation of all the modes of magnetostrictive deformation. Here we are only interested in the CF origin irreducible strains, preserving the axial symmetry:¹ $\epsilon^{\alpha,1} = \epsilon_{xx} + \epsilon_{yy} + \epsilon_{zz}$, the volume distortion, and $\epsilon^{\alpha,2} = (\sqrt{6}/2)[\epsilon_{zz} - (1/3)\epsilon^{\alpha,1}]$, the shape variation only along the c axis (ϵ_{ij} are the Cartesian strains). In Figs. 1 and 2 we show the really quite complex temperature dependencies for the measured spontaneous strains $\epsilon^{\alpha,1}$ and $\epsilon^{\alpha,2}$ (Refs. 2 and 8), obtained when the spontaneous magnetization rotates from the easy basal plane towards the applied field direction, i.e., $\mathbf{H} \parallel \mathbf{c}$, the hard axis.⁹

The interest of the present study stems from several considerations: the number of noncubic $3d$ intermetallic compounds with Y, La, or Lu, where magnetostriction has been measured in single crystals or sintered pseudocrystals is quite reduced;¹⁴ in contrast with the only theoretically investigated cubic Ni metal,⁵ within the BKF scheme, magnetostrictive strains in the uniaxial Y_2Fe_{17} system are somehow larger than in Ni (and in Fe as well¹⁵), an advantage for comparing with theoretical

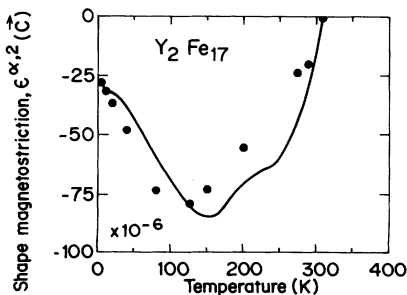


FIG. 2. As in Fig. 1, but for the c/a axial tetragonal irreducible distortion $\epsilon^{\alpha,2}$, for the Y_2Fe_{17} intermetallic compound (Refs. 2 and 8). The determined microscopic magnetoelastic coupling parameter M_{22}^{α} is quoted in Table I.

calculations. Such large strains should be sought in the stronger CEF produced by the Y^{3+} nearest-neighbor ions surrounding the dumbbell of the $4f$ Fe atoms.

Our task here is double: to explain the complex temperature dependencies of the $\epsilon^{\alpha,1}$ and $\epsilon^{\alpha,2}$ modes, and as an important by-product to determine the second-order microscopic MEL coupling coefficients. The paper is organized in the following way: in Sec. II we introduce the system Hamiltonian and obtain its energy levels; in Sec. III we develop a detailed presentation of the magnetostriction model for uniaxial systems; in Sec. IV we account for the results, and in Sec. V we discuss our work and extract the main conclusions.

II. MODEL HAMILTONIAN AND ENERGY LEVELS CALCULATION

A. The model Hamiltonian

Our calculations are done within the tight-binding approximation (although this approximation is not essential for the model), using Bloch functions of the usual kind,

$$\psi_{\lambda}(\mathbf{k}; \mathbf{r}) \equiv |\mathbf{k}; \lambda\rangle = \frac{1}{\sqrt{N}} \sum_l e^{i\mathbf{k} \cdot \mathbf{l}} \phi_{\lambda}(\mathbf{r} - \mathbf{l}), \quad (1)$$

where \mathbf{l} are the Fe atom positions, \mathbf{k} the wave vector, λ stands for the atomic orbital plus spin states and N is the number of Fe atoms in the crystal. $\phi_{\lambda} \equiv |\lambda\rangle$ are atomic wave functions, product of the orbital basis $|1\rangle$ to $|5\rangle$ times the spinors, and a common radial, $f(r)$, function.

The $3d$ itinerant electron Hamiltonian H at site \mathbf{l} is modeled in the following way:^{1,10}

$$H = H_{CF} + H_z^S + H_z^L + H_{so} + H_{me} + H_{el}, \quad (2)$$

where the different Hamiltonian terms are as follows underneath. All they refer to a unique ion: i.e., they are translationally invariant. It is shown that such invariance means that matrix elements of H are of the form $\langle \mathbf{k}'; \lambda' | H | \mathbf{k}; \lambda \rangle = \langle \lambda' | H | \lambda \rangle \delta_{\mathbf{k}, \mathbf{k}'}$, i.e., \mathbf{k} independent. Therefore we can treat H as a localized-electron Hamiltonian. For the CF term we will initially take the one for $3m$ point symmetry,

$$H_{CF} = \sum_{n=2,4} B_{no} \bar{O}_{no} + B_{43} \bar{O}_{43}, \quad (3)$$

where B_{nm} are CF coefficients and \bar{O}_{nm} and \bar{O}_{nm} , orbital angular momentum L , Stevens-Buckmaster-type operators.¹⁶ In particular,

$$\begin{aligned} \bar{O}_{20} &= L_z^2 - (1/3)L(L+1), \\ \bar{O}_{40} &= 35L_z^4 - [30L(L+1) - 25]L_z^2 \\ &\quad + 3L(L+1)[L(L+1) - 2]. \end{aligned}$$

We will neglect the nonaxial CF term in (3) because the basal plane anisotropy is negligible in Y_2Fe_{17} (Ref. 9), the ensuing Hamiltonian having the full hexagonal symmetry (point group $6/m, 2/m, 2/m$). This approximation is compatible with the $4f$ -site $3m$ -point symmetry of the magnetostrictive atoms. Within the $\{|1\rangle, |2\rangle\}$, $\{|3\rangle, |4\rangle\}$, and $|5\rangle$ orbital basis, inclusion of remainder

terms $B_{20}\tilde{O}_{20} + B_{40}\tilde{O}_{40}$ gives the splitting, $\Delta_{20} + 4\Delta_{40} - (2\Delta_{20} + \Delta_{40})$, $2\Delta_{20} - 6\Delta_{40}$, with $\Delta_{20} \equiv -\alpha_L B_{20} \langle r^2 \rangle_{3d}$ and $\Delta_{40} = -\beta_L (B_{40}/12) \langle r^4 \rangle_{3d}$, where α_L, β_L are Stevens reduced matrix elements and $\langle r^n \rangle_{3d}$, the Fe 3d shell radial n moment.¹⁶ Notice that the perturbed energy level gravity center remains invariant as $Tr\{\tilde{O}_n^m\} = 0$ ($m, n \neq 0$).¹⁶ Nothing is known about the values of the CF parameters for Y_2Fe_{17} , which turns out to a determination of the CF level splitting, currently unfeasible. Therefore, they must be adjusted within our magnetostriction calculation, and in order to reduce the number (eight) of adjustable parameters in our calculation we will make the further simplifying approximation of keeping only $B_{20}\tilde{O}_{20}$ within the CF Hamiltonian. We will see that such an approximation works quite well when comparing our model results with magnetostriction experiments.

The Zeeman term is composed of spin and orbital contributions, which within the mean-field approximation and under an effective magnetic field of exchange origin, \mathbf{H}_{eff} (the external field is considered zero, inasmuch as we are going to calculate spontaneous strictions), can be written as

$$H_z^S = -\mu_B (\boldsymbol{\sigma} + \alpha \mathbf{L}) \cdot \mathbf{H}_{\text{eff}}, \quad (4)$$

where $\boldsymbol{\sigma}$ are the Pauli matrices and α a parameter, which takes into account the effective quenching by the CF of the orbital angular momentum \mathbf{L} , and also the effect of the orbital polarization by H_{eff} , likely through spin-spin and spin-orbit interactions. However, a clear understanding of the origin of such a polarization has not yet been fully achieved.¹⁷ The spin-orbit contribution has the usual form,

$$H_{so} = A \mathbf{L} \cdot \boldsymbol{\sigma}, \quad (5)$$

where A is the spin-orbit coupling constant.

The CF single-ion magnetoelastic coupling Hamiltonian, up to second-order terms, has the form¹

$$H_{me} = - \sum_{i=1,2} \left[M_{i1}^\alpha [L_x^2 + L_y^2 + L_z^2] \epsilon^{\alpha,i} + \frac{\sqrt{3}}{2} M_{i2}^\alpha [L_z^2 - \frac{1}{3} L(L+1)] \epsilon^{\alpha,i} \right], \quad (6)$$

$\mathbf{H}_{\text{eff}} \parallel c$ (OX axis) :

$$\langle 1, \mp 1/2 | H_z^{S+L} | 1, \pm 1/2 \rangle = \langle 2, \pm 1/2 | H_z^{S+L} | 2, \mp 1/2 \rangle = -\mu_B H_{\text{eff}}^x, \quad (9a)$$

$$\langle 5 | H_z^{S+L} | 5 \rangle = -\mu_B H_{\text{eff}}^x, \quad (9b)$$

where $H_z^{S+L} \equiv H_z^S + H_z^L$.

$\mathbf{H}_{\text{eff}} \parallel c$ (OZ axis) :

$$\langle 1, \pm 1/2 | H_z^{S+L} | 1, \pm 1/2 \rangle = \mp \mu_B H_{\text{eff}}^z, \quad \langle 2, \pm 1/2 | H_z^{S+L} | 1, \pm 1/2 \rangle = -i \mu_B \alpha H_{\text{eff}}^z, \quad (10a)$$

$$\langle 5, \pm 1/2 | H_z^{S+L} | 5, \pm 1/2 \rangle = \mp \mu_B H_{\text{eff}}^z. \quad (10b)$$

Now, according to Eq. (6), the MEL Hamiltonian is diagonal and, for both spin projections (except for a common factor \hbar^2), becomes

where M_{ij}^α ($i, j = 1, 2$) are the *microscopic* MEL coupling coefficients and $\epsilon^{\alpha,i}$, the irreducible strains defined in Sec. I.

Finally the classical elastic energy for hexagonal systems, keeping only the terms related to the α strains, is¹

$$H_{el} = \frac{1}{2} [C_{11}^\alpha (\epsilon^{\alpha,1})^2 + C_{22}^\alpha (\epsilon^{\alpha,2})^2] + C_{12}^\alpha \epsilon^{\alpha,1} \epsilon^{\alpha,2}. \quad (7)$$

B. Hamiltonian matrix elements and energy levels calculation

The H_{CF} Hamiltonian diagonal matrix elements have already been considered in Sec. II A. Accordingly with the model outlined in Sec. II, for the Zeeman spin and orbit Hamiltonians we have to consider two situations, either the spontaneous magnetization (i.e., the effective magnetic field) being along the c axis or within the basal plane, and besides to obtain the matrix elements of the MEL Hamiltonian (6). Now, in order to simplify the calculations, we have neglected the matrix elements of the spin-orbit interaction between the two doublets and between these doublets and the singlet. This approximation is justified if the crystal-field energy is much greater than the spin-orbit coupling one, which is the case here. In this way, a nonzero orbital magnetic moment for our model system is formed only within the two doublets. Then the only nonzero matrix elements for both spin projections are

$$\begin{aligned} \langle xz, \pm 1/2 | H_{so} | yz, \pm 1/2 \rangle \\ = \langle yz, \mp 1/2 | H_{so} | xz, \mp 1/2 \rangle = \pm i A, \\ \langle x^2 - y^2, \pm 1/2 | H_{so} | xy, \pm 1/2 \rangle = \mp 2i A. \end{aligned} \quad (8)$$

We will treat both strains $\epsilon^{\alpha,1}$ and $\epsilon^{\alpha,2}$ on the same foot because the MEL Hamiltonians in (6) are identical, except for the MEL coupling coefficients. This is reasonable because both strain modes preserve the unit cell hexagonal symmetry. Consider, for instance, the modifying c/a ratio strain $\epsilon^{\alpha,2}$ and cast together the spin and orbital Zeeman Hamiltonians. We obtain the same matrix elements for the two doublets, and if, e.g., we consider the doublet $\{|1\rangle, |2\rangle\}$, we have for \mathbf{H}_{eff} applied either perpendicular or parallel to the hard c axis the following.

$$\begin{aligned}
\langle 1|H_{me}^{\alpha,2}|1\rangle &= \langle 2|H_{me}^{\alpha,2}|2\rangle = - \left[6M_{21}^{\alpha} - \frac{\sqrt{3}}{2}M_{22}^{\alpha} \right] \epsilon^{\alpha,2}, \\
\langle 3|H_{me}^{\alpha,2}|3\rangle &= \langle 4|H_{me}^{\alpha,2}|4\rangle = -(6M_{21}^{\alpha} + \sqrt{3}M_{22}^{\alpha})\epsilon^{\alpha,2}, \\
\langle 5|H_{me}^{\alpha,2}|5\rangle &= -(6M_{21}^{\alpha} - \sqrt{3}M_{22}^{\alpha})\epsilon^{\alpha,2}.
\end{aligned} \tag{11}$$

As it was said before, the matrix elements involved in the volume strain, $\epsilon^{\alpha,1}$, calculation are identical to the above ones, just changing, in Eqs. (11), M_{21}^{α} and M_{22}^{α} by M_{11}^{α} and M_{12}^{α} , respectively. The diagonalization of Hamiltonian (2) (making use of the above matrix elements) yields the eigenvalues underneath, which split the $\{|1\rangle, |2\rangle\}$, $\{|3\rangle, |4\rangle\}$, and $|5\rangle$ energy levels in the form.

$\mathbf{H}_{\text{eff}} \perp \mathbf{c}$:

$$E_{1,2} = E_{3,4} = \pm \sqrt{(\mu_B H_{\text{eff}}^x)^2 + A^2} + \Delta + \left[-6M_{21}^{\alpha} + \frac{\sqrt{3}}{2}M_{22}^{\alpha} \right] \epsilon^{\alpha,2}, \tag{12a}$$

$$E_{5,6} = E_{7,8} = \pm \sqrt{(\mu_B H_{\text{eff}}^x)^2 + 4A^2} - 2\Delta - (6M_{21}^{\alpha} + \sqrt{3}M_{22}^{\alpha})\epsilon^{\alpha,2}, \tag{12b}$$

$$E_{9,10} = \pm \mu_B H_{\text{eff}}^x + 2\Delta + (-6M_{21}^{\alpha} + \sqrt{3}M_{22}^{\alpha})\epsilon^{\alpha,2}. \tag{12c}$$

$\mathbf{H}_{\text{eff}} \parallel \mathbf{c}$:

$$E'_{\{3,4\}} = \mp \mu_B H_{\text{eff}}^z \pm (A \mp \alpha_1 \mu_B H_{\text{eff}}^z) + \Delta + \left[-6M_{21}^{\alpha} + \frac{\sqrt{3}}{2}M_{22}^{\alpha} \right] \epsilon^{\alpha,2}, \tag{13a}$$

$$E'_{\{7,8\}} = \mp \mu_B H_{\text{eff}}^z \pm (2A \mp 2\alpha_1 \mu_B H_{\text{eff}}^z) - 2\Delta - (6M_{21}^{\alpha} + \sqrt{3}M_{22}^{\alpha})\epsilon^{\alpha,2}, \tag{13b}$$

$$E'_{9,10} = \mp \mu_B H_{\text{eff}}^z + 2\Delta + (-6M_{21}^{\alpha} + \sqrt{3}M_{22}^{\alpha})\epsilon^{\alpha,2}. \tag{13c}$$

In Eq. (13a), the upper and lower signs in front of the first term and inside the second term correspond to the new (1,2) and (3,4) doublets respectively, and the signs in front of the second terms split those energy levels, fully lifting the degeneracy. The same rules apply to Eq. (13b). In the case of the volume strain mode, $\epsilon^{\alpha,1}$, the energy levels obtained are, indeed, identical to those in Eqs. (12) and (13), if we modify the MEL coupling coefficients in the form above mentioned.

A calculation entirely identical to the done above, shows that for the $\{|xy\rangle, |x^2-y^2\rangle\}$ doublet, the Zeeman Hamiltonian matrix elements are similar, except that now the orbital quenching constant α can be, in principle, different.

The energy levels (12) and (13), constitute the centers for the energy bands in the distorted crystal, before to consider any itineracy effects or energy band \mathbf{k} dispersion. This aspect will be treated in the next section, which constitutes the core of the present model.

III. MAGNETOSTRICTION MODEL FOR UNIAXIAL ITINERANT SYSTEMS

The model presented here is an extension of an early model developed for isotropic and cubic symmetry systems,^{10,11} as it was mentioned before. Nevertheless we will now develop with more detail some of the previously obtained results, for the sake of transparency and also because the obtention of the irreducible strains is more complex.

It is a well-known result^{6,7} that the main contribution

to magnetic anisotropy and magnetoelastic coupling comes from those regions of the Brillouin zone (BZ) where symmetry is high enough. This simplifies the problem of anisotropy and magnetostriction calculations enormously, because such regions are in fact reduced to a few \mathbf{k} points of high symmetry in the BZ. Besides, in order to have any anisotropy and magnetostriction, those states must be degenerate or nearly so, as we have seen in Sec. II. This degeneration is lifted out by the strong spin and orbit Zeeman interactions and by the, in comparison, weaker spin-orbit coupling, which is relatively small in 3d transition metals and intermetallics. An additional condition must be fulfilled, and it is that the energy of those high-symmetry Bloch states should be close enough to the Fermi level. This condition is required because within our approach, the orbital magnetic moment is not quenched for the states in those \mathbf{k} regions, and it is completely quenched elsewhere. This quenching is well known to be due to interband site hopping because the Slater-Koster integral matrix elements for the hopping Hubbard t_{ij} operator vanish by symmetry in the above-mentioned regions of the BZ.¹⁸

Our basis of one-electron states, in order to build the Bloch functions (1), is limited here to the ten 3d states obtained in Sec. II B, at high-symmetry points of the BZ, plus two nonorbital states with spins up and down, coming from band electrons of other characters. An even further simplification is to consider only a single \mathbf{k} point in the BZ: either for the 4f site or for the whole hexagonal cell, the BZ will have uniaxial symmetry. Then some particular \mathbf{k} point within the axis and close to the Fermi

wave vector \mathbf{k}_F would likely be the most important in determining the magnetic anisotropy and magnetoelastic coupling interaction. The above assumed two nonorbital states will not give any contribution to the magnetoelastic coupling, i.e., their energies will not depend on the strain. Then, our model function for the density of states consists of ten narrow bands plus two wide bands, all of them approximated by symmetrical elliptical functions but with different bandwidths and filling capacities. The centers of those narrow bands have been already determined and are given by Eqs. (12) and (13). The energy positions of the wide bands are determined by the spin Zeeman term only. Now, the energy of the system is calculated within the Stoner model,¹⁹ i.e.,

$$U = \sum_{\lambda} \int_{-\infty}^{\mu} E \rho_{\lambda}(E) dE, \quad (14)$$

where $\rho_{\lambda}(E)$ is the density of states of the λ th subband and given by the expression,

$$\rho_{\lambda}(E) = \frac{2C_{\lambda}}{\pi W_{\lambda}} \left[1 - \left[\frac{E - E_{\lambda}}{W_{\lambda}} \right]^2 \right]^{1/2}. \quad (15)$$

C_{λ} and W_{λ} are the filling capacities and the half bandwidth of the λ th subband, respectively, μ is the chemical potential, and E_{λ} are the λ -subband energy centers, given by Eqs. (12) and (13). A constraint in the model is, indeed, the condition of the constant number of $3d$ electrons n within the ten subbands, where

$$n_{\lambda} = \int_{-\infty}^{\mu} \rho_{\lambda}(E) dE \quad (16)$$

is the λ th subband number of electrons and

$$\sum_{\lambda} n_{\lambda} = n, \quad (17)$$

the constraint, which in turn determines the chemical potential μ , which becomes temperature dependent when the spontaneous magnetization (or H_{eff} , proportional to it) varies, as we shall see.

Our final goal is the calculation of the irreducible equilibrium spontaneous strains $\epsilon^{\alpha,1}$ and $\epsilon^{\alpha,2}$, in special their temperature dependencies, for which we have experimental data at hand for the Y_2Fe_{17} intermetallic compound^{2,8} as was mentioned before. The calculation will be performed within the rigid-band model.²⁰ It means that changes of shape of the density of states $\rho_{\lambda}(E)$ due to the magnetization (of orbital and spin origins) and, to a lesser extent, to the deformation of the crystal, are neglected. Therefore, within our model description the effect of the magnetization (or of H_{eff}) and the strains on the electronic structure is limited to mutual shifts of particular subbands. Temperature effects on the irreducible strains are taken into account through the temperature variation of H_{eff} , or equivalently of the system spontaneous magnetization.¹⁰ We will now describe in some more detail such calculations, which were early outlined in Ref. 10.

Under the external solicitation (effective field and/or strain) each subband λ should shift in $\Delta E_{\lambda}(H_{\text{eff}}, \epsilon^{\alpha,i})$ under the rigid-band hypothesis. Therefore, the Fermi level

has to change, by $\Delta\mu$, in order to fulfill the constraint (17), or equivalently $\sum_{\lambda} \Delta n_{\lambda} = 0$, where Δn_{λ} is the λ th subband electron occupation variation due to the shift. This variation, within the linear approximation for ΔE_{λ} , assumed to be small enough, amounts,

$$\Delta n_{\lambda} = \rho_{\lambda}(\mu) \Delta\mu - \rho_{\lambda}(\mu) \Delta E_{\lambda}, \quad (18)$$

which under the above constraint yields,

$$\Delta\mu(H_{\text{eff}}, \epsilon^{\alpha,i}) = \frac{\sum_{\lambda} \rho_{\lambda}(\mu) \Delta E_{\lambda}}{\sum_{\lambda} \rho_{\lambda}(\mu)}. \quad (19)$$

Now, the overall energy variation of the system is,

$$\Delta U(H_{\text{eff}}, \epsilon^{\alpha,i}) = \sum_{\lambda} (\Delta U_{\lambda}^{(1)} + \Delta U_{\lambda}^{(2)} + \Delta U_{\lambda}^{(3)}), \quad (20)$$

where each term in (20) has the following expression and meaning: $\Delta U_{\lambda}^{(1)} = -n_{\lambda} \Delta E_{\lambda}$ is the energy subband gain under a rigid-band shift, $\Delta U_{\lambda}^{(2)} = \mu \rho_{\lambda}(\mu) \Delta E_{\lambda}$ is the energy subband cost in order to keep the chemical potential μ the same for all polarized subbands, and $\Delta U_{\lambda}^{(3)} = -\mu \Delta\mu \rho_{\lambda}(\mu)$ is the energy subband gain due to the modification of μ . Through the introduction of (19) in (20) and using the energy variations $\Delta U_{\lambda}^{(i)}$, shows that contributions $i=2$ and 3 cancel out, and therefore, the net energy variation finally amounts to

$$\Delta U(H_{\text{eff}}, \epsilon^{\alpha,i}) = - \sum_{\lambda} n_{\lambda} \Delta E_{\lambda}. \quad (21)$$

This result means that, for a given spontaneous magnetization (or H_{eff}), Eq. (21) gives the magnetoelastic energy of the system, which becomes temperature dependent through the modification of the Stoner gap $\delta = (M_+ - M_-) H_{\text{eff}}$, where M_{\pm} are the up and down spin plus orbital magnetizations in the direction of \mathbf{H}_{eff} and $M_S(T) \equiv M_+ - M_-$ is the spontaneous magnetization. Notice that Eq. (21) keeps in well with the rigid-band assumption, where the effect of the magnetization and strain is limited to the mutual shifts of particular subbands, although generally electron transfer among them does occur.

Now, for a constant value of M_S (or H_{eff}), if \mathbf{H}_{eff} is applied parallel and perpendicular to the c axis, the energy difference

$$U_K \equiv U(\mathbf{H}_{\text{eff}} \parallel c) - U(\mathbf{H}_{\text{eff}} \perp c) \quad (22)$$

[where U is given by Eq. (14)] represents the magneto-crystalline anisotropy energy of the system, which for an easy-plane system as Y_2Fe_{17} , must be a positive quantity. Such a constraint was imposed to our calculation of the magnetostrictive strains, as it will be shown in Sec. III.

Now the MEL energy given by Eq. (21) is a macroscopic one, and we should relate it to the phenomenological MEL energy expression for uniaxial systems, in terms of Callen and Callen¹ phenomenological MEL coupling constants $\bar{M}_{ij}^{\Gamma}(H_{\text{eff}}, T)$ and irreducible strains. The MEL expression can be obtained from the microscopic Hamiltonian (6), in the form,¹

$$U_{me} = -[\bar{M}_{11}^{\alpha} \epsilon^{\alpha,1} + \bar{M}_{21}^{\alpha} \epsilon^{\alpha,2}] (\alpha_1^2 + \alpha_2^2 + \alpha_3^2) - \frac{\sqrt{3}}{3} [\bar{M}_{12}^{\alpha} \epsilon^{\alpha,1} + \bar{M}_{22}^{\alpha} \epsilon^{\alpha,2}] [\alpha_3^2 - \frac{1}{2}(\alpha_1^2 + \alpha_2^2)], \quad (23)$$

where $(\alpha_1, \alpha_2, \alpha_3)$ are the cosine directions of the spontaneous magnetization, \mathbf{M}_s (or of \mathbf{H}_{eff}). In order to relate Eqs. (21) and (23) to obtain the phenomenological MEL coupling parameters, we proceed to calculate the strain derivatives of both expressions and to equate them.¹⁰ However, in order to isolate the individual MEL parameters we have to consider the energy differences for \mathbf{H}_{eff} parallel and perpendicular to the c axis, in the case of the $\epsilon^{\alpha,1}$ and $\epsilon^{\alpha,2}$ modes. Proceeding in such a way we immediately obtain for the phenomenological MEL parameters the expression,

$$\bar{M}_{i2}^{\alpha} = \sqrt{3} \left[\left(\sum_{\lambda} n_{\lambda} \frac{\partial E_{\lambda}}{\partial \epsilon^{\alpha,i}} \right)_{\mathbf{H}_{\text{eff}} \parallel c} - \left(\sum_{\lambda} n_{\lambda} \frac{\partial E_{\lambda}}{\partial \epsilon^{\alpha,i}} \right)_{\mathbf{H}_{\text{eff}} \perp c} \right], \quad (24)$$

with $i=1,2$. Notice that these parameters have been calculated within our rigid-band assumption, i.e., changes of the shape of the density of states due to the existence of spontaneous magnetization and to the strains are neglected. It means that, within our model, the influence of magnetization and strains on the electronic structure is limited to mutual shifts of particular subbands, as said before. On the other hand, in order to obtain the equilibrium irreducible strains we have to add to (23) the elastic energy (7) and minimize the overall energy, obtaining in such a way, for the equilibrium strains,

$$\epsilon^{\alpha,1}(c) = \frac{\sqrt{3}}{3} \frac{\bar{M}_{12}^{\alpha}}{C_{11}^{\alpha}}, \quad \epsilon^{\alpha,2}(c) = \frac{\sqrt{3}}{3} \frac{\bar{M}_{22}^{\alpha}}{C_{22}^{\alpha}}, \quad (25)$$

where C_{ij}^{α} are the symmetric elastic stiffness constants. The strictions (25) correspond to the spontaneous magnetization along the hard c axis, which were the actual measured irreducible strains for Y_2Fe_{17} compound.² In the derivation of Eqs. (25) we have assumed that the different strain modes are decoupled, i.e., each time the other strain is assumed to be zero, which is, in fact, the experimental result.^{2,9} Equations (24) and (25) represent the goal of our model.

IV. RESULTS

In Figs. 1 and 2, respectively, we present the experimental temperature dependencies for the spontaneous magnetostriction models $\epsilon^{\alpha,1}$ and $\epsilon^{\alpha,2}$ (Refs. 2 and 8). These values were obtained from the magnetostriction vs applied magnetic field isotherms at the anisotropy field values H_K (of the order of 3T along the c axis), where the rotational magnetization process against the anisotropy torques is finished.⁹ This field is indeed negligible compared with the molecular one and was neglected in the evaluation of H_{eff} . In Fig. 3 we show the calculated temperature variation of the reduced magnetocrystalline anisotropy energy $U_K(T)/U_K(0)$, according to Eqs. (22) and (14). The positive sign of this energy was used to con-

trol that the basal plane was the easy one, at all temperatures. In Figs. 1 and 2 we also represent the achieved theoretical fits for the irreducible strictions temperature variations, calculated according to Eqs. (24) and (25). As overall, the fits can be reputed as reasonably good. Nothing is known about the Cartesian elastic stiffness constants C_{ij} for Y_2Fe_{17} intermetallic compound, but considering that this compound is an iron-rich one, we have taken for C_{ij} the values for pure iron.²¹ At 0 K, they amount $C_{11} = 2.41 \times 10^{11} \text{ J m}^{-3}$ and $C_{12} = 1.46 \times 10^{12} \text{ J m}^{-3}$, being very weakly temperature dependent. Then the relevant symmetry elastic constants for uniaxial symmetry, approximately are¹

$$C_{11}^{\alpha} = \frac{2}{9}[C_{11} + C_{12}], \quad C_{22}^{\alpha} = \frac{2}{3}[C_{11} + C_{12}], \quad (26)$$

and then $C_{11}^{\alpha} = 0.86 \times 10^{10} \text{ J m}^{-3}$ and $C_{22}^{\alpha} = 2.56 \times 10^{10} \text{ J m}^{-3}$, being very slightly temperature dependent between 0 K and $T_C \cong 310 \text{ K}$. The values of the model parameters used in the above strain fits are collected in Table I. The value of Δ was slightly different ($\cong 4\%$) for the fits of $\epsilon^{\alpha,1}$ and $\epsilon^{\alpha,2}$. We fixed the total number of electrons within the whole band to $n = 7.2$ per Fe atom,²² and the 0-K Stoner gap δ was taken from the polarized band-structure calculations of Inoue and Shimizu.²² δ was allowed to vary with temperature according with the spontaneous magnetization M_S temperature variation.¹⁰ We allowed also the chemical potential μ to vary with temperature, as we explained before, in order to keep n constant.

The second major result, which emerges from our work is the determination of the *microscopic* magnetoelastic coupling parameters M_{12}^{α} and M_{22}^{α} . The values obtained from the above fits are quoted in Table I. They are large (between around one and two orders of magnitude larger) when comparing with many strongly anisotropic rare-earth intermetallics,²³ as could be expected for a $3d$ shell transition element intermetallic compound.

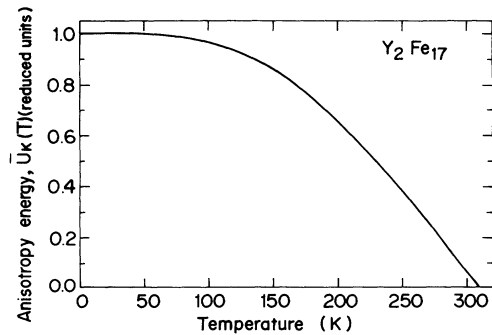


FIG. 3. Temperature dependence of the calculated reduced magnetocrystalline anisotropy energy $\bar{U}_K(T) = U_K(T)/U_K(0)$ [see Eq. (22) in text], for the Y_2Fe_{17} intermetallic compound. The sign of U_K is positive at all temperatures.

TABLE I. Values for the model parameters used for the Y_2Fe_{17} intermetallic compound. The meaning of the parameters is the following: R is the ratio between the filling capacities of the wide conduction and the five d -electron narrow bands; Δ is the axial crystal-field energy shift for the $\{xy, yz\}$ doublet; W_0 is the half-band width of the wide conduction electron band; W_1 , the half-band width for the $3d$ narrow bands; n is the total number of $3d$ electrons per Fe (Ref. 22); δ is the Stoner gap (Ref. 22); α is the orbital quenching and polarization parameter; A is the spin-orbit coupling parameter (Ref. 5); M_{12}^α and M_{22}^α are the determined *microscopic* magneto-elastic coupling parameters (in degrees K per Fe atom).

R	Δ (eV)	W_0 (eV)	W_1 (eV)	n	δ (eV)	α	A (eV)	M_{12}^α	M_{22}^α
1	1.23 ^a 1.28 ^b	3.4	0.3	7.2	1.266	0.4	0.0468	-1.4×10^3	-0.8×10^3

^aFrom the fitting of the $\epsilon^{\alpha,1}$ mode thermal variation (Refs. 2 and 8).

^bFrom the fitting of the $\epsilon^{\alpha,2}$ mode thermal variation (Refs. 2 and 8).

V. DISCUSSION AND CONCLUSIONS

A model of magnetostriction for uniaxial itinerant ferromagnets has been developed, which gives a good account for the magnetoelastic behavior of the hexagonal iron-rich intermetallic compound Y_2Fe_{17} . In our model calculations, some strong approximations have been made, which do not allow us to consider the present results as fully quantitative ones. The most important of them are the model density of states, taking into account only one point of the Brillouin zone, the neglecting of some matrix elements of the spin-orbit Hamiltonian, the description of the complex axial crystal field (CF) potential by only one adjustable second-order CF parameter and the lack of thermal excitations. Still, we believe that our phenomenological description reflects the essential features of the CF origin magnetoelastic coupling for the Y_2Fe_{17} hexagonal intermetallic compound. If first-principles electronic structure calculations were performed to obtain the magnetoelastic coupling parameters, they should be based on the same physical picture of the coupling of the crystal-lattice electric field to the spins through the anisotropic $3d$ orbital states.

The main achievements of this work are as follows. First of all, the fits of the complex temperature dependencies of the volume $\epsilon^{\alpha,1}$ and c/a distortion $\epsilon^{\alpha,2}$ irreducible strains (or equivalently of the \bar{M}_{12}^α and \bar{M}_{22}^α phenomenological magnetoelastic parameters) for the Y_2Fe_{17} hexagonal ferromagnet. Such strictions, of pure crystal-field origin, could not be certainly explained within the localized electron picture.¹ Second is the determination, for such uniaxial system, of the *microscopic* magnetoelastic coupling parameters M_{12}^α and M_{22}^α , respectively, related with the $\epsilon^{\alpha,1}$ and $\epsilon^{\alpha,2}$ strains. These parameter values are summarized in Table I. The large values obtained (between one and two orders of magnitude larger than for strongly anisotropic rare-earth intermetallics) indicate, as expected, the strong crystal-field potential felt by the $3d$ shell atoms in intermetallic compounds with Y or a rare-earth partner. To our knowledge this is the first time that such *microscopic* parameters are obtained for a uniaxial intermetallic compound, having as magnetic atoms a $3d$ element only.

In order to fit the temperature dependencies of the anisotropic α -striction modes we keep the CF Hamiltonian

only up to second order, using only a single CF parameter Δ , and we modify it very slightly (about 4%) in order to fit the thermal dependence of the two modes $\epsilon^{\alpha,1}$ and $\epsilon^{\alpha,2}$. It can be shown that the phenomenological MEL coupling parameters, calculated according to Eqs. (24), are extremely sensitive to rather small variations in Δ (around 10^{-3}). This means that the simple approach to magnetostriction for itinerant electron ferromagnets, developed in Sec. III, looks quite reliable.

The thermal dependence of the irreducible strictions (or equivalently of the phenomenological magnetoelastic parameters) was treated through their dependence on the Stoner gap, which is believed to be proportional to the spontaneous magnetization.²⁰ The Stoner model is known to fail in the description of collective thermal excitations.^{20,24} However, we would like to stress here that we do not calculate the temperature dependence of the magnetization. Instead, we use the experimental variation of this dependence, to compare the calculated Stoner gap variation of the magnetostriction with the measured thermal dependence of the irreducible magnetostrictive strains. We should also add that the Stoner model has been found to be equivalent to the more rigorous local-spin-density approximation.¹⁹ The essential difference between these two approaches is the energy dependence of the Stoner gap. However, this dependence is not crucial here because the main contribution to the magnetoelastic coupling comes from narrow-band states, whose energies are near to the Fermi level.

ACKNOWLEDGMENTS

One of the authors (K.K.) is grateful to the Spanish Ministry of Education and Science for financial support from the program "Profesor en Año Sabático" and to the CAI-CONAI of Aragón for a grant of stay at the University of Zaragoza. A.d.M. is grateful to Professor P. M. Etxenike and to Dr. J. González for their hospitality at the Universidad del País Vasco/Euskal Herriko Unibertsitatea (San Sebastián/Donostia). Discussions with Berta García-Landa about experimental magnetostriction results are warmly acknowledged. This work was partially supported by Project No. 2P-302 031 04 from the Polish Science Research Council and by the Spanish DGICYT under grant PB90-1014.

- *On leave from the Faculty of Physics and Nuclear Techniques, University of Mining and Metallurgy, 30059 Cracow, Poland.
- ¹E. R. Callen and H. B. Callen, *Phys. Rev.* **129**, 578 (1963); E. R. Callen *ibid.* **139**, A455 (1965).
- ²B. García-Landa, M. R. Ibarra, P. A. Algarabel, F. E. Kayzel, T. H. Anh, and J. J. M. Franse, *Physica B* **177**, 227 (1992).
- ³P. A. Algarabel, A. del Moral, M. R. Ibarra, J. B. Sousa, J. M. Moreira, and J. F. Montenegro, *J. Magn. Magn. Mater.* **69**, 285 (1987).
- ⁴P. A. Algarabel, A. del Moral, M. R. Ibarra, and C. Marquina, *J. Magn. Magn. Mater.* **114**, 161 (1992).
- ⁵H. Brooks, *Phys. Rev.* **58**, 909 (1940); T. Katayama, *Sci. Rep. Res. Inst. Tohoku Univ. A* **3**, 341 (1951); G. C. Fletcher, *Proc. Phys. Soc. A* **67**, 505 (1954); **68**, 1066 (1955).
- ⁶E. I. Kondorskii and E. Straube, *Zh. Eksp. Teor. Fiz.* **63**, 356 (1972) [*Sov. Phys. JETP* **36**, 188 (1973)].
- ⁷N. Mori, *J. Phys. Soc. Jpn.* **27**, 307 (1969); N. Mori, Y. Fukuda, and T. Ukai, *ibid.* **37**, 1263 (1974).
- ⁸A. del Moral, in *Magnetoelastic Effects and Applications*, edited by L. Lanotte (Kluwer, Amsterdam, 1993), p. 1.
- ⁹S. Sinnema, Ph.D. thesis, University of Amsterdam, 1988 (unpublished), and references therein.
- ¹⁰K. Kulakowski and E. T. de Lacheisserie, *J. Magn. Magn. Mater.* **81**, 349 (1989).
- ¹¹K. Kulakowski and J. Wenda, *J. Magn. Magn. Mater.* **94**, 247 (1991); K. Kulakowski, A. Maksymowicz, and M. Magdon, *ibid.* **115**, L143 (1992).
- ¹²D. Givord, Ph.D. thesis, University of Grenoble, 1973 (unpublished).
- ¹³D. Givord, R. Lemaire, J. M. Moreau, and E. Roudaut, *J. Less Common Met.* **29**, 361 (1972).
- ¹⁴See for instance, A. V. Deryagin, N. V. Kudrevatykh, R. Z. Levitin, and Yu. F. Popov, *Phys. Status Solidi B* **68**, K163 (1975); A. V. Andreev, A. V. Deryagin, S. M. Zadvorkin, and S. V. Terent'ev, *Fiz. Tverd. Tela (Leningrad)* **27**, 1641 (1985) [*Sov. Phys. Solid State* **27**, 987 (1985)]; A. del Moral, P. A. Algarabel, and M. R. Ibarra, *J. Magn. Magn. Mater.* **69**, 285 (1987).
- ¹⁵W. J. Carr, in *Handbuch der Physik*, edited by S. Flüge (Springer-Verlag, Berlin, 1966), p. 274.
- ¹⁶M. T. Hutchings, *Solid State Phys.* **16**, 227 (1964); H. A. Buckmaster, *Can. J. Phys.* **40**, 1670 (1962).
- ¹⁷O. Eriksson, B. Johansson, R. C. Albers, A. M. Boring, and M. S. S. Brooks, *Phys. Rev. B* **42**, 2707 (1990).
- ¹⁸J. C. Slater and G. F. Koster, *Phys. Rev.* **94**, 1498 (1954).
- ¹⁹See, for instance, F. Gautier, in *Magnetism of Metals and Alloys*, edited by M. Cyrot (North-Holland, Amsterdam, 1982).
- ²⁰D. Wagner, *Introduction to the Theory of Magnetism* (Pergamon, New York, 1972), p. 227.
- ²¹E. P. Wohlfarth, in *Ferromagnetic Materials*, edited by E. P. Wohlfarth (North-Holland, Amsterdam, 1980), Vol. 1, p. 3.
- ²²J. Inoue and M. Shimizu, *J. Phys. F* **15**, 1511 (1985).
- ²³M. R. Ibarra and A. del Moral, *J. Magn. Magn. Mater.* **83**, 121 (1990); A. del Moral, M. R. Ibarra, P. A. Algarabel, and J. I. Arnaudas, in *Physics of Magnetic Materials*, edited by W. Gorzkowski, M. Gutowski, H. K. Lachowicz, and H. Szymczak (World Scientific, Singapore, 1991), p. 90.
- ²⁴D. C. Mattis, *The Theory of Magnetism* (Harper & Row, New York, 1965), p. 211; R. M. White, *Quantum Theory of Magnetism* (McGraw-Hill, New York, 1970), p. 175.